1-1-2013

Multifunctional conducting fibres with electrically controlled release of ciprofloxacin

Dorna Esrafilzadeh
University of Wollongong, de256@uowmail.edu.au

Joselito M. Razal
University of Wollongong, jrazal@uow.edu.au

Simon E. Moulton
University of Wollongong, smoulton@uow.edu.au

Elise M. Stewart
University of Wollongong, elises@uow.edu.au

Gordon G. Wallace
University of Wollongong, gwallace@uow.edu.au

Multifunctional conducting fibres with electrically controlled release of ciprofloxacin

Abstract

We hereby present a new method of producing coaxial conducting polymer fibres loaded with an antibiotic drug that can then be subsequently released (or sustained) in response to electrical stimulation. The method involves wet-spinning of poly(3,4-ethylenedioxythiophene) poly(styrenesulfonate) (PEDOT:PSS) fibre, which served as the inner core to the electropolymerised outer shell layer of polypyrrole (Ppy). Ciprofloxacin hydrochloride (Cipro) was selected as the model drug and as the dopant in the Ppy synthesis. The release of Cipro in phosphate buffered saline (PBS) from the fibres was controlled by switching the redox state of Ppy.Cipro layer. Released Cipro under passive and stimulated conditions were tested against Gram positive (Streptococcus pyogenes) and Gram negative (Escherichia coli) bacteria. Significant inhibition of bacterial growth was observed against both strains tested. These results confirm that Cipro retains antibacterial properties during fibre fabrication and electrochemically controlled release. In vitro cytotoxicity testing utilising the neural B35 cell line confirmed the cytocompatibility of the drug loaded conducting fibres. Electrical conductivity, cytocompatibility and tuning release profile from this flexible fibre can lead to promising bionic applications such as neuroprosthetics and localised drug delivery.

Keywords

multifunctional, conducting, ciprofloxacin, fibres, release, electrically, controlled

Disciplines

Engineering | Physical Sciences and Mathematics

Publication Details

Esrafilzadeh, D., Razal, J. M., Moulton, S. E., Stewart, E. M. & Wallace, G. G. (2013). Multifunctional conducting fibres with electrically controlled release of ciprofloxacin. Journal of Controlled Release, 169 (3), 313-320.

Multifunctional conducting fibres with electrically controlled release of Ciprofloxacin

Dorna Esrafilzadeh, Joselito M. Razal, Simon E. Moulton, Elise M. Stewart and Gordon G. Wallace*

ARC Centre of Excellence for Electromaterials Science and
Intelligent Polymer Research Institute, University of Wollongong
Wollongong, NSW 2522, Australia

Abstract

We hereby present a new method of producing coaxial conducting polymer fibres loaded with an antibiotic drug that can then be subsequently released (or sustained) in response to electrical stimulation. The method involves wet-spinning of poly(3,4-ethylenedioxythiophene) poly(styrenesulfonate) (PEDOT:PSS) fiber, which served as the inner core to the electropolymerised outer shell layer of polypyrrole (Ppy). Ciprofloxacin hydrochloride (Cipro) was selected as the model drug and as the dopant in the Ppy synthesis. The release of Cipro in phosphate buffer saline (PBS) from the fibres was controlled by switching the redox state of Ppy.Cipro layer. Released Cipro under passive and stimulated conditons were tested against Gram positive (*Streptococcus pyogenes*) and Gram negative (*Escherichia coli)* bacteria. Significant inhibition of bacterial growth was observed against both strains tested. These results confirm that Cipro retains antibacterial properties during fibre fabrication and electrochemically controlled release. *In vitro* cytotoxicity testing utilising the neural B35 cell line confirmed the cytocompatibility of the drug loaded conducting fibres. Electrical conductivity, cytocompatibility and tuning release profile from this flexible fibre can lead to promising bionic applications such as neuroprosthetics and localised drug delivery.

Keywords: Inherently conducting polymer, fibre-spinning, Ciprofloxacin hydrochloride, drug delivery

*Corresponding author: Prof. Gordon. G. Wallace, Email: gwallace@uow.edu.au

Phone: +61-2–4221 3127, Fax: +61-2-4221 3114

1. Introduction

Advances in the fabrication of neuroprosthetic electrodes have attracted considerable interest from biomedical researchers [1-5]. These electrodes can be incorporated into a neuroprosthetic device capable of electrically stimulating cells as well as recording signals generated by cells [6]. Electrodes can be fabricated into a range of geometries including pads, cuffs or longitudinal intra-fascicular electrodes [2, 7, 8].

Critical to the successful application of any electrode *in vivo* is their biocompatibility, stable conductivity, low impedance, appropriate mechanical properties and flexibility [4]. In addition, a major factor in implantable device failure is associated with post-surgery infection [9]; therefore developing an electrode with inherent anti-inflammatory or antibiotic features is highly attractive [10]. Prevention of infection following the implantation can be addressed by the incorporation and controlled release of specifically targeted drugs that can be used singularly, or in combination into neuroprosthetic electrodes [10, 11].

There exists today a wide range of drug delivery formulations such as polymeric microparticles and implants [12-14], with some structures capable of triggering release in response to discrete thermal transitions [14, 15], pH [16, 17] or electrical stimuli [18, 19]. Electrically stimulated drug delivery systems have the advantage of tuning the release

profile by the nature of the stimulation conditions (the current/potential magnitude and frequency) employed [20]. Consequently, electrical stimulation to affect localised and controlled release of therapeutic drugs is becoming an attractive option in the treatment of acute disease or chronic illness [11].

So far, inherently conducting polymers (ICPs) are being utilised in the fabrication of electrode structures for the primary purpose of recording cellular activities[13], as well as having the secondary role of responding to electrical stimulation to initiate drug release [21, 22]. The lower electrochemical impedance of ICPs, compared to metal electrodes, if combined with an appropriately sized biomolecule/drug, leads to their efficient release via electrical stimulation[6]. For example, it has been demonstrated that dexamethasone (DEX) can be effectively released from neural microelectrode surface covered by poly(3,4-ethylenedioxythiophene) (PEDOT) [5]. The electrically stimulated release of the neurotrophin NT-3 from polypyrrole has also been reported [20, 23, 24]. Recently, dexamethasone (an anti-inflammatory drug) and penicillin and streptomycin (antibiotics) have been incorporated into polypyrrole (Ppy) [25] whilst dexamethasone has also been incorporated into poly(3,4-ethylenedioxythiophene) (PEDOT) [11] and released using electrical stimulation.

To date, most of the ICP based drug delivery systems have been limited to electropolymerised films as stand alone materials or as coatings on other (usually rigid) substrates [26, 27]. However, the drawbacks associated with the use of ICP films including their brittleness, inflexibility, need for structural support and competent charge carrier (i.e. gold mylar) and the delamination from support substrate during redox processes have severly affected thier use in drug delivery systems [1, 2]. In contrast, ICP fibres can provide self-supporting three-dimensional, flexible architectures suitable for *in vitro* and *in vivo* bionic applications [1, 2]. ICPs can also allow the incorporation and controlled release of chemical or biochemical triggers (drugs, growth factors) [26]. Recently, highly conducting PEDOT:PSS fibres produced by wet-spinning method have been shown to posses stable electrochemical properties [28]. To the best of our knowledge, ICP microfibre structures have not been previously used to develop intelligent drug delivery systems.

Here, we present a novel method to produce coaxial ICP fibres wherein electrically controlled release of the antibiotic ciprofloxacin hydrochloride is achievable. PEDOT:PSS-chitosan hybrid fibres were fabricated employing a novel wet-spinning strategy involving the coagulation of PEDOT:PSS using chitosan as the coagulant. The hybrid fibre was subsequently used as a working electrode for the electropolymerisation of a ciprofloxacin hydrochloride doped Ppy layer (Ppy.Cipro). The PEDOT:PSS-chitosan core acts as structural support and electronic conductor to electrochemically switch Ppy.Cipro between reduced and oxidised states to controllably release (or sustain) Cipro. The bioactivity of the released antibiotic drug (Cipro) was evaluated *in vitro.* Furthermore, the cytotoxicity of the fibres and their components was tested against a neural cell model.

2. Experimental

Materials and methods

2.1. Materials

Poly(3,4-ethylenedioxythiophene) poly(styrenesulfonate) (PEDOT:PSS) pellets were obtained from Agfa (Orgacon dryTM, Lot A6 0000 AC). Chitosan (CHI) with high molecular weight (MW) was supplied from Sigma with 75 % rate of deacetylation. Ciprofloxacin hydrochloride (Cipro) was obtained from MP Biomedical Inc. (Lot No. of 8460H) with MW=367.84 g mol^{-1}. Ethylene glycol (EG) Reagent Plus ≥ 99% solution was purchased from

Sigma-Aldrich (Batch No. of 04397JJ). Pyrrole monomer was obtained from Merck and was distilled prior to use. Deionised Milli-Q water (18 MΩ cm^{-1}) was used to prepare all aqueous solutions. The release of ciprofloxacin hydrochloride was measured in Phosphate Buffered Saline (PBS) solution with pH≈ 7.4 prepared by dissolving standard PBS tablet (Merck, Germany) in 1 litre water. Glacial acetic acid was purchased from Sigma and diluted to 2.0 wt. %.

2.2. Instrumentation

Wet-spinning of the fibres was performed using custom-made wet-spinning equipment. Fibre post-spinning treatment was carried out by wetting the fibres with ethylene glycol (EG) followed by oven drying at 120 °C for 1 hr to improve the conductivity [28-30]. Electropolymerisation of pyrrole monomer was performed galvanostatically in a three-electrode cell (working, reference and counter electrode) using an eDAQ (Australia) potentiostat/galvanostat run by eDAQ Chart™ software version 5.2. Electrically stimulated release of Ciprofloxacin hydrochloride was performed in a three electrode cell. The cyclic voltammogram of the conducting materials was measured using an eDAQ (Australia) potentiostat/galvanostat running Echem software version 1.5. The morphology of the fibres was imaged using field emission scanning electron microscope (FESEM) JEOL7500 at specific voltage of 5 kV and Optical Leica Microscopy model DMED controlled by Leica software version (2.4.0 R1). The energy-dispersive X-ray spectroscopy (EDX) was performed using FESEM JEOL7500 microscope. Raman spectra (laser wavelength used was 623 nm) were obtained using a Jobin Yvon Horiba HR800 Raman spectrometer with Lab Spec software.

2.3. Wet-spinning of PEDOT:PSS-CHI hybrid fibres

A PEDOT:PSS dispersion (25 mg/ml) in water was homogenised (10,000 rpm for 10 min) and bath sonicated (1 h) to prepare the spinning solution. The PEDOT:PSS dispersion was then loaded into a 5 ml syringe with a detachable needle (20 gauge) as the spinneret. The feed rate of PEDOT:PSS was fixed at 15 ml/h using a syringe pump (KDS-Scientific 100). The PEDOT:PSS dispersion was injected into the chitosan coagulation bath (1.0 wt. % chitosan dissolved in 2.0 wt. % acetic acid) to form an ionic cross-linked gel fibre, which was then washed in an ethanol bath before collection on a spool (Fig. S1). Dried PEDOT:PSS-CHI fibres were treated with ethylene glycol (EG) followed by heating to 120 °C for 30 min to increase the conductivity of the hybrid fibres [31].

2.4. Electrochemical characterisation of PEDOT:PSS-CHI fibres

In order to investigate the electrochemical behaviour of hybrid PEDOT:PSS-CHI fibres, cyclic voltammerty was performed in PBS. Conductivity of the fibres was measured using a linear four-point probe conductivity cell with uniform 2.3 mm spacing between probes. A galvanostat current source (Princeton Applied research Model ED402) and digital multimeter (HP Agilent 34401A) were used to obtain conductivity. Electrochemistry measurements including cyclic voltammetry of the fibres were performed in a three-electrode cell, using a potentiostat as described above with software of EChem version 1.5. The electrochemical impedance spectroscopy (EIS) was carried out in a two-electrode cell in PBS electrolyte using Gamry Instruments Framework (V.5.5).

2.5. Synthesis of Ppy.Cipro layer on the surface of PEDOT:PSS-CHI fibres

Synthesis of polypyrrole doped with ciprofloxacin hydrochloride (Ppy.Cipro) was performed galvanostatically in a glass vial containing a platinum mesh (counter electrode), an Ag/AgCl

reference electrode and a PEDOT:PSS-CHI fibre as the working electrode (Fig. S2). The length of fibre was 3 cm, however, only 1 cm of the fibre was inserted into the polymerisation solution. The polymerisation solution contained 0.2 M pyrrole monomer and 50 mM ciprofloxacin hydrochloride in Milli-Q water. Two different current densities (0.5 and 2.0 mA/cm^2) with different growth times (10 and 20 min) were applied. All current densities were normalised by thickness and geometric surface area of the fibres to achieve a similar thickness of Ppy.cipro layer for each current density and time point. All fibres were washed in Milli-Q water for 5 min after electropolymerisation to remove any unincorporated Cipro on the surface of fibres.

2.6. Scanning Electron Microscopy

All images of coaxial fibres were taken using field emission scanning electron microscopy (FESEM) (JEOL JSM-7500FA). Samples for cross-section imaging were prepared by breaking a frozen fibre after dipping into liquid nitrogen. Samples were sputter-coated (EDWARDS Auto 306) with a thin layer of platinum (~3 nm thickness) prior to imaging.The chemical elements present in the surface and cross section of PEDOT:PSS-CHI fibres were investigated using Energy-Dispersive X-ray Spectroscopy (EDX). In this case, the presence of sulphur (PEDOT:PSS) was monitored using FESEM and EDX simultaneously.

2.7. Elemental Analysis.

Elemental analysis for nitrogen (N) and sulphur (S) in the PEDOT:PSS-CHI fibres was determined using an automatic analyser (Carlo Erba 1106) technique at the Australian National University (ANU, Canberra). Four different samples were examined including dry PEDOT:PSS powder, dry chitosan powder, a PEDOT:PSS-CHI film prepared by blending solutions of PEDOT:PSS and chitosan (1% w/v) at a ratio of 9:1 and PEDOT:PSS-CHI fibres.

2.8. Mechanical property testing

The tensile properties of the fibres were measured using a Shimadzu EZ-S at a strain rate of 0.5 % min^{-1}. Samples were mounted on aperture cards (1 cm length window) with commercial super glue and allowed to air dry. Young's modulus, tensile strength and breaking strain were calculated and the mean and standard deviation reported for n = 10.

2.9. Ciprofloxacin (Cipro) release measurement

The amount of released Cipro was determined via UV.vis spectroscopy by monitoring the absorption of Cipro at its λmax 270 nm in PBS. The UV.vis spectra of PBS solutions containing Cipro at varying concentrations were recorded between 200 nm and 300 nm using a Shimadzu UV 1601 spectrophotometer in order to construct an absorbance/concentration calibration curve for sample analysis (Fig. S3-A). No other component of the fibre absorbs at this wavelength, therefore eliminating any possible interference with compounds other than Cipro (Fig. S3-B). Loading efficiency of Cipro per 1 cm length of fibre was estimated by dissolving 1 cm length of fibre in PBS solution. The drug loaded fibre was bath sonicated for 5 days until the fibre completely dissolved and the Ppy.Cipro coating broke down, then the solution was filtered and the Cipro concentration was obtained by UV.vis spectroscopy. To monitor the effect of sonication on the absorption properties of Cipro, control solutions of known concentrations of Cipro in PBS were treated under the same conditions as the fibres. The release medium was collected by micropipette at specific time points over 3 days and replaced with the same volume of fresh PBS solution. All cumulative release data are plotted

as a percentage of (M_t) release relative to the Cipro loading (M_{tot}). Cipro release was investigated under passive diffusion and electrical stimulation conditions (applied constant potential) in different stimulation patterns. In the first one, constant potential (reduced or oxidised) was applied to fibres during 72h (Fig 4) whilst, in the second pattern, the alternative constant potential was applied by switching between reduced and oxidised potential every 24 h for 72 h (Fig S8) For electrically stimulated release, a platinum mesh and Ag/AgCl electrode were utilised as the counter electrode and the reference electrode, respectively whilst the PEDOT:PSS-CHI-Ppy.Cipro fibre was the working electrode. The release solution was gently stirred with constant speed during the release experiments to assist diffusion of Cipro from the surface of the fibres. Fibres with consistent lengths and thicknesses were chosen as test samples.

2.10. Antibacterial activity of released Ciprofloxacin

The activity of the Ciprofloxacin hydrochloride released from the fibres was tested against both Gram-negative *Escherichia coli* (JM109) and Gram-positive *Streptococcus pyogenes* (NS5448). Bacterial lawns were prepared by firstly inoculating 5 ml of Luria-Bertani (LB) medium or Todd Hewitt (TH) broth with *E. coli* or *S. pyogenes* respectively for overnight incubation at 37 °C. This culture was then used to inoculate a 10 ml culture which was grown to mid-log phase (OD_{600} 0.6-0.8; determined using an Ultrospec10 spectrophotometer). This culture was then diluted 1/5 in sterile 0.9 % (w/v) NaCl in Milli-Q and 200 µl of this suspension was spread onto LB or TH agar plates. The bacterial suspension was air dried prior to application of either fibres or discs. Following fibre production, dried fibres were prepared in 1cm lengths for antibacterial testing. To test the efficacy of Cipro released from fibres, lengths were carefully placed onto the surface of the prepared plates which were then inverted and incubated at 37 °C overnight prior to examination. Both PEDOT:PSS-CHI and PEDOT:PSS-CHI-Ppy.Cl fibres were tested as controls to ensure no antibacterial activity was exhibited by other components of the fibres. The bioactivity of Cipro released from the fibres either passively or under electrical stimulation was also tested. The fibres were placed in 500 µL PBS for 72 h. Release samples were then loaded onto sterile 6 mm discs of Whatman No.1 filter paper and allowed to air dry at room temperature. The loaded discs were then carefully placed onto prepared bacterial plates. Discs placed on *E. coli* lawns were loaded with 10 µl of release media, and discs placed on *S. pyogenes* lawns were loaded with 20 µl of release media to account for the different susceptibilities of the bacterial strains to Cipro. Control discs were also prepared by preloading with 1 µg of ciprofloxacin hydrochloride for efficacy comparisons.

2.11. Cytotoxicity testing

The cytotoxicity of PEDOT:PSS-CHI, PEDOT:PSS-CHI-Ppy.Cl and PEDOT:PSS-CHI-Ppy.Cipro fibres were tested against B35 neuroblastoma cell line (ATCC). Cells were cultured in DMEM medium supplemented with 10 % (v/v) fetal bovine serum (FBS, Invitrogen). The composite fibres were aligned on glass slide substrates and 8-well cell culture chamber was glued onto the substrate to immobilise the fibres at the substrate surface. The fibre surfaces were sterilised by rinsing in 70 % (v/v) ethanol followed by air drying. The fibres in each well were coated with Type IV rat tail collagen by exposing the surface to 50 µg/ml collagen prepared in 0.02 % acetic acid solution for 1 h at room temperature. Wells were then rinsed twice in serum free medium prior to cell seeding at a density of 10,000 cells/cm^2. Cells were incubated at 37 °C in a humidified 5 % CO_2 environment for 48 h prior to staining and imaging. Cells were stained for metabolic activity by the addition of Calcein AM (Invitrogen) to the a final concentration of 1 µg/ml in cell culture media, followed by

incubation as above for 15 min. Propidium iodide (Invitrogen) was then added to final concentration of 1 µg/ml and the cells incubated for 5 min at room temperature. Medium was then removed and replaced with fresh PBS prior to imaging with an AxioImager fitted with a Mrm AxioCam and images were overlayed using AxioVision Software (Zeiss). An LDH release assay was also performed to determine the IC50 for Cipro against B35 cells. B35 cells were seeded at a density of 5,000 cells/well into a 96 well plate. Following 24 h incubation as described above, cell media was replaced with complete media containing a dilution series of Cipro starting at the highest concentration of 1 mg/ml. Following 48 h incubation cell media was collected and assayed for LDH activity using the CytoTox 96® Non-Radioactive Cytotoxicity Assay (Promega).

3. Results and discussion

3.1. Wet-spinning of PEDOT:PSS-CHI fibres

Polyionic complexation coagulation strategy was employed to wet-spin PEDOT:PSS fibres. PEDOT:PSS dispersion (25 mg/ml) was injected into a chitosan (CHI) coagulation bath. Based on the polyionic complexation coagulation strategy [32], the "free" negatively charged polystyrene sulphonate acid (PSS) groups of PEDOT:PSS can react with positively charged amino group of chitosan to form a gel fibre. Different concentrations of CHI (from 0.5 to 2 wt. %) were used as the coagulation bath. PEDOT:PSS fibres could not be coagulated at CHI concentrations less than 1 wt. %. The spinability of PEDOT:PSS fibres improved significantly at CHI concentrations higher than 1 wt. %. However, the high viscosity of CHI coagulation bath at concentrations higher than 2 wt. % hindered the spinability of PEDOT:PSS fibres. In order to minimise the adverse effects of CHI uptake on the electrical conductivity of the resultant fibre, the minimum CHI concentration (1 wt. %) needed for effective spinning was chosen as the coagulation bath. The gel fibre was then dehydrated and washed in an ethanol bath to remove the unreacted CHI from the surface of the fibre. In contrast to solvent/non-solvent as-spun PEDOT:PSS fibres [28], PEDOT:PSS-CHI fibres were insoluble and stable in aqueous media (pH ≃ 7.4) due to present of insoluble chitosan in pH ≃ 7.4 and polyionic complexation between chitosan and PEDOT:PSS which facilitates their use in bionic applications.

The elemental composition of the fibres was evaluated using energy-dispersive X-ray (EDX) spectroscopy. The EDX spectrum showed sulphur peaks which confirmed the presence of PEDOT:PSS on the surface of fibre. However, the cross-sectional EDX suggested a hybrid structure of PEDOT:PSS-CHI fibre where the inner part is rich in PEDOT:PSS and the outer layer is rich in chitosan (Fig. S4). Elemental analysis was carried out to measure the ratio of chitosan to PEDOT:PSS in the as-dried hybrid fibre. Based on the percentage of nitrogen from chitosan and sulphur from PEDOT:PSS in the control samples (Table S1), a calibration curve was used to determine the ratio of chitosan to PEDOT:PSS. The composition was calculated to be 3.23% to 96.77%, respectively. Such a low mass ratio of chitosan is favourable as it shows lower negative impact on the electrical conductivity of the hybrid fibre.

SEM images of the "as-spun" hybrid fibre is shown in Fig. 1A. The hybrid fibre was dense and non-porous with a smooth surface and a circular cross section (diameter = 65 ± 7 µm) upon drying under tension. This circular cross section was obtained over a wide range of spinning parameters.

The electrochemical behavior of the fibres was investigated using cyclic voltammetry (CV) using PEDOT:PSS-CHI hybrid fibres as the working electrode in PBS buffer. Ethylene

glycol (EG) post-treated spun fibres exhibited well defined electrochemical responses corresponding to oxidation and reduction of the PEDOT backbone (Fig. 1D). The improved electrochemistry after EG treatment is attributed to a change in the conducting polymer conformation from a compact coil to an extended coil configuration followed by phase separation between excess PSS and PEDOT [28-30, 33]. The currents recorded in the CV did not change noticeably after 100 cycles confirming the electrochemical stability of the fibre (Fig. S5). The conductivity of EG-treated fibres measured by the four point probe method was 56 ± 7 S cm^{-1}.

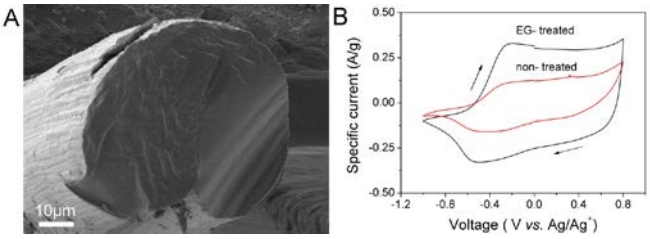

Fig. 1. SEM image of PEDOT:PSS-CHI fibre (A), Cyclic voltammogram of PEDOT:PSS-CHI fibre in PBS (pH ~ 7.4) between -1.0 V and +0.8 V at scan rate of 50 mV/s (B). Arrows indicate the direction of potential scan.

3.2. Electropolymerisation of Ppy.Cipro on PEDOT:PSS-CHI fibre.

The electrical and electrochemical properties of the EG-treated PEDOT:PSS-CHI fibres demonstrated high electrical conductivity and stable electrochemistry in aqueous media. Therefore, this fibre was chosen as a micro-dimensional electrode onto which a drug loaded polypyrrole (Ppy) conducting polymer was electrochemically polymerised. The drug selected was ciprofloxacin hydrochloride (Cipro), a synthetic chemotherapeutic antibiotic of the fluoroquinolone drug class [34]. Electropolymerisation of Ppy.Cipro onto the PEDOT:PSS-CHI fibre was performed galvanostatically in a monomer solution of 0.2 M pyrrole and 50 mM ciprofloxacin hydrochloride at current densities (0.5 and 2.0 mA/cm^2) and polymerisation times (10 and 20 min). The concentration of monomer was selected on the basis of previously published work as several studies have been performed with same concentration of pyrrole monomer [20]. The isoelectric point of ciprofloxacin is 7.4 [35], therefore Cipro possesses a positive charge at the pH used for the polymerisation (pH ≃ 4.7). We propose that the negative chloride ion (Cl^-) from the ciprofloxacin hydrochloride acts as the dopant for the Ppy and the Cipro is physically entrapped as the polymer grows. This entrapment mechanism has been previously reported by our group for the encapsulation and controlled release of the positively charged neurotrophin-3 (NT-3) using Ppy [20, 24]. The total amount of Cipro loaded into a 1cm length (254±13 µg) of fibre was determined to be 42±4 µg/cm. When the Ppy.Cipro polymer was grown on the PEDOT:PSS-CHI fibre, the oxidation potential generated was between +0.28 to +0.45 V at all investigated current densities. These oxidation potentials are much lower than the oxidation potential observed when Ppy.Cipro was synthesised on a gold mylar surface (+0.8V) which allowed us to ensure the Ppy layer was not over oxidised during polymerisation [26].

SEM images of Ppy.Cipro polymerised on one end of the PEDOT:PSS-CHI fibre is shown in Fig. 2. The Ppy.Cipro shows a fibrillar morphology, which is significantly different to the usual "cauliflower" morphology of Ppy reported in the literature even when synthesised at a higher current density (2.0 mA/cm^2) with extended polymerisation time (20 min) [20]. We believe that the PEDOT:PSS-CHI substrate structure facilitates the fibril formation. We propose that when the PEDOT:PSS-CHI fibre is placed in the monomer solution, the fibre

swells to form the fine fibril features and as the Ppy.Cipro forms, it locks in this fibril structure. The mechanical properties of PEDOT:PSS-CHI-Ppy.Cipro fibres were enhanced compared to their as-spun counterparts. Modulus, strength and breaking strain of PEDOT:PSS-CHI-Ppy.Cipro fibres, obtained from stress- strain curves, were calculated to be 2.9 ± 0.2 GPa, 128 ±11 MPa, 30.5 ± 4 %, respectively (Fig. 3A). The as-dried EG-treated PEDOT:PSS-CHI fibres displayed modulus, strength and breaking strain of 2 ± 0.3 GPa, 99 ± 7 MPa, 20.6 ± 1.2 %, respectively.

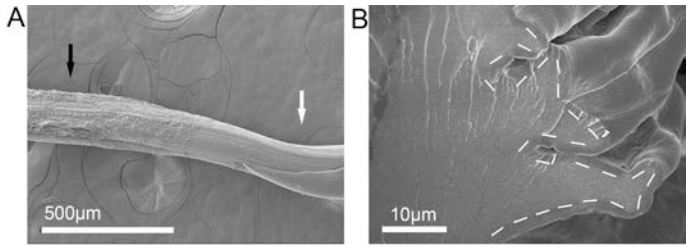

Fig. 2. SEM images of PEDOT:PSS-CHI fibre after electropolymerisation of the Ppy.Cipro second layer (A) (arrows show polymerised (black) and uncoated (white) ends), cross section of Ppy.Cipro end (B) (the white dashed line is included to aid the reader in observing the Ppy.Cipro layer). The current density used to polymerise the Ppy.Cipro layer was 2mA/cm^2 and the polymerisation time was 10 min.

The Ppy.Cipro layer is observed in Fig. 2B as the thin dense layer at the surface of the PEDOT:PSS-CHI fibre (indicated with a partial dashed line). The thickness of this layer was determined from the SEM images and the relationship between current density, polymerisation time and thickness of the Ppy.Cipro layer is shown in Table 1. The thickness of Ppy.Cipro layer increases as both current density and polymerisation time increase. These results suggest that the pyrrole monomer does not penetrate into the PEDOT:PSS-CHI fibre structure due to the non-porous morphology of the fibre and decreased wet ability after EG treatment.

Table 1. Oxidation potential and thickness of Ppy.Cipro layer as a function of polymerisation condition. The thickness was determined from SEM images.

Current density (mA/cm^2)	Polymerisation time (min)	Thickness of Ppy.Cipro layer (µm)	Oxidation potential (V)
2.0	20	1.9± 0.1	0.45
2.0	10	1.3± 0.3	0.45
0.5	20	1.4± 0.1	0.33
0.5	10	0.5± 0.1	0.28

Raman spectra were recorded between 800 and 1700 cm^{-1} to probe the changes that have occurred at the molecular level after second layer deposition (Fig. 3B). Comparison of band positions before and after polymerisation confirmed formation of a Ppy.Cipro layer. For the PEDOT:PSS-CHI fibre, peaks were observed at 1530 cm^{-1} (C=C stretching), 1426 cm^{-1} (C=C stretching), 1366 cm^{-1} (C-C stretching) and 1257 cm^{-1} (C=C stretching) with these assignments based on reports by others [28]. Whereas, spectra of the PEDOT:PSS-CHI-Ppy.Cipro fibre and Ppy.Cipro film (control) both showed a strong sharp peak in 1580 cm^{-1} (C=C stretching) , a double peak at 1320 and 1380 cm^{-1} (ring stretching) and peaks in 927 and 1240 cm $^{-1}$ (C-H out of plane bending) indicative of the oxidised form of Ppy [26]. Transformation of the Raman vibration properties from PEDOT:PSS to Ppy after electropolymerisation of the second layer confirms formation of Ppy layer onto fibre substrate. However, changes in Raman spectra depend on the thickness of the Ppy layer and time of polymerisation. It is worth noting that after polymerisation of longer than 10 min the

Ppy.Cipro layer was thick enough to avoid penetration of Raman laser into PEDOT:PSS-CHI layer.

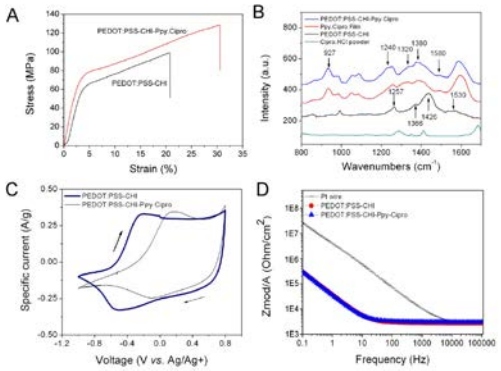

Fig. 3. Stress-strain curves of PEDOT:PSS-CHI and PEDOT:PSS-CHI-Ppy.Cipro fibres (A). Raman spectra of Ppy.Cipro grown on PEDOT:PSS-CHI fibre (B). Cyclic voltammogram of PEDOT:PSS-CHI fibre at PBS (pH ≃ 7.4) between -9.0 V and +0.8V at scan rate of 25 mV/s before and after electropolymerisation of Ppy.Cipro layer (current density: 2.0 mA/cm^2 & polymerisation time: 10 min). Arrows indicate the direction of potential scan (C) and electrochemical impedance spectroscopy of wet-spun fibres in comparison to Pt wire (D).

Electrochemical testing of the PEDOT:PSS-CHI fibres (Fig. 3C) shows oxidation and reduction peaks of at -0.3 V and -0.5 V, respectively. Upon Ppy.Cipro polymerisation, the oxidation and reduction peaks shifted to +0.2V (oxidation) and -0.1V (reduction) and were found to be stable when thick Ppy.Cipro layer was achieved (ie. polymerisation time: 10 min). This redox behaviour was similar to that of a Ppy.Cipro film grown on gold mylar, suggesting these redox peaks were due to the Ppy.Cipro polymer. The oxidation and reduction peak potential of the Ppy.Cipro is +0.2V and -0.1V respectively. These redox values are at potentials higher than the oxidation state of the PEDOT:PSS fibre core.(-0.2V) This provides the possibility to switch between oxidised and reduced state for Ppy.Cipro layer whilst the PEDOT:PSS layer remains in its oxidised state (conducting state). This is very important as the PEDOT:PSS core can act as a conduit for charge delivery during different redox state of drug loaded Ppy.Cipro outer layer.

Fig. 3D showed lower impedance of the PEDOT:PSS-CHI-Ppy.Cipro (~2.8 kΩ/cm^2) at 1 kHz (relevant frequency of biological activities) [5] in comparison to platinum wire (~ 10.3 kΩ/cm^2). This improved impedance resulted from facilitating penetration of ions which provide much higher electroactive surface area compared to the Pt wire due to the gel-like nature of the hybrid fibre. Moreover, the impedance of fibres did not change after polymerisation of Ppy.Cipro.

3.3. Ciprofloxacin release

The release of the entrapped Cipro from the Ppy.Cipro layer was performed under passive and electrical stimulation conditions in PBS (pH ≃ 7.4) at 37 ^{o}C in a three electrode cell as described in the experimental section. A 1 cm length of PEDOT:PSS-CHI-Ppy.Cipro fibre was placed in PBS with samples taken at various time intervals. Electrically stimulated release was performed under potentials that induced an oxidised (+0.3 V *vs* Ag/AgCl) and reduced (-0.26 V *vs* Ag/AgCl) state in the Ppy.Cipro layer. These potentials were chosen from the PEDOT:PSS-CHI-Ppy.Cipro CV shown in Fig. 3C. The passive release of Cipro showed short term release for the first 8 h followed by a plateau up to 72 h (Fig. 4). These

results suggest that under passive conditions, Cipro release is dominated by diffusion of near-surface trapped Cipro. According to the Raman data (Fig. 3B) and high electrical conductivity of the fibres, the Ppy.Cipro layer is in its conducting state; therefore Ppy tends to keep its dopant to balance the charge along the polymer backbone to maintain neutral charge. As the interaction between dopant and polymer comes from electrostatic forces, passive Cipro release is predominantly the result of drug that is near the surface or loosely trapped within the layer.

The stimulated release profiles of Cipro from the Ppy.Cipro layer of the PEDOT:PSS-CHI-Ppy.Cipro fibre are shown in Fig. 4. When the PEDOT:PSS-CHI-Ppy.Cipro fibre is electrically stimulated, so that the Ppy.Cipro layer is in the oxidised state, the release profile is very similar to the passive release. The main difference is that in the oxidised state, the amount of Cipro release has decreased. When a reducing potential is applied to the PEDOT:PSS-CHI-Ppy.Cipro fibre, longer term sustained release up to 72 h is observed with approximately 2 times higher concentration of released drug compared to the passive mode.

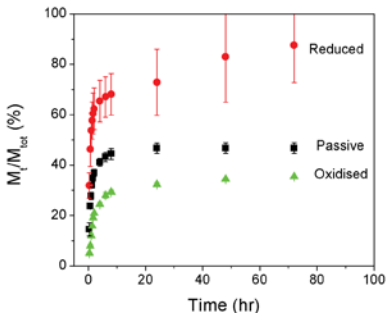

Fig. 4. Cumulative release profile of Cipro from PEDOT:PSS-CHI-Ppy.Cipro fibres in different conducting states up to 72 h. The percentage of drug amount (M_t) released relative to drug loading (M_{tot}) from fibres. The release experiments were carried out in PBS (pH ≃ 7.4) at 37 ^{o}C. Error bars indicate the standard error of the mean (n = 3).

By reducing Ppy.Cipro, an excess negative charge is placed along the polymer backbone, in order to balance this charge the polymer can either release its negatively charged Cl^- dopant or incorporate cations from the media it is residing in. We have previously shown that Cl^- ions are very mobile and are readily expelled upon Ppy electrochemical reduction [36]. As the dopant is expelled, so is the drug that was physically entrapped during synthesis as reported before for NT-3 delivery [24]. It has previously been shown that the dopant plays an important role in determining the extent of release of the entrapped drug [37]. In the oxidised state around 20 % less Cipro is released in comparison to passive during 72 h. When the Ppy.Cipro is further oxidised, the polymer posses a positive charge and therefore the Cl^- dopant is retained within the Ppy.Cipro layer. It is likely that the positive charge is balanced by uptake of negative ions from the PBS solution. However, from Fig. 4 it is clear that upon oxidation Cipro release is observed, albeit not to the same degree as when in the passive or reduced state. In addition, the release experiments have been carried out by switching between reduced and oxidised potential of Ppy.Cipro layer and shown the capability of fibres to tune release profile in different redox state of conducting polymer (Fig. S8). The control of release demonstrated here based on charge application highlights the versatility of our fibres for drug delivery systems. The mechanism for Cipro release is proposed to involve electrostatic interactions as the application of electrical stimulation protocol varied the amount of Cipro release. However, both the ionic and hydrophobic properties of polypyrrole have been shown to vary upon application of electrical stimulus. The expansion and contraction (actuation) [26] of polypyrrole is also a well-documented property of polypyrrole

upon oxidation and reduction and these processes may be involved in the release of Cipro. As all of these properties change simultaneously it is not possible to separate them to determine which process is the dominant factor driving this release.

3.4. In vitro antibacterial efficacy

The previous section clearly demonstrates that it is possible to incorporate and release Cipro from the coaxial fibre in a controlled manner. However, it is important to evaluate whether the Cipro maintains its antibacterial properties during the fabrication process. The formation of a zone of inhibition (ZOI) within a lawn of bacteria was used to evaluate the efficacy of released Ciprofloxacin. A ZOI represents inhibition of the growth of an organism within a designated zone corresponding to the presence of an active substance. In this study, the ZOI of Cipro was determined for representative Gram-positive and Gram-negative bacteria. Firstly, the drug loaded and control fibres were applied to lawns of each bacterial strain. A ZOI was observed surrounding the drug loaded fibres (Fig. 5A & 5C) placed on lawns of each bacterial strain, but not surrounding the underlying PEDOT:PSS fibre, nor the Ppy coated Cl-doped fibres. These results confirm that the inhibition of bacterial growth was solely due to the presence of ciprofloxacin in these fibres. The absence of a ZOI surrounding the control fibres (PEDOT:PSS-CHI and PEDOT:PSS-CHI-Ppy.Cl) shows that the components of these fibres do not display any antibacterial effect. The inhibition of bacterial growth indicates that the associated processing steps required to prepare these fibres do not adversely affect the bioactivity of the ciprofloxacin under passive release conditions. Moreover, the amount of drug loaded and subsequently released from the fibre under passive conditions was sufficient to diffuse through the agar media to affect bacterial growth. Secondly, the effect of the method of Cipro release from the fibres on its efficacy was investigated (Fig. 5B & 5D). Cipro-containing media collected after 72 h of cumulative release was loaded onto bacterial lawns via paper discs. The release medium obtained following application of electrical stimulation, at both oxidising and reducing potential, resulted in maintained antibacterial activity, which indicates that electrical stimulation did not disrupt drug biological activity. This study importantly confirms that Cipro maintains its bioactivity against both Gram-positive and Gram-negative bacteria during loading via electrochemical polymerisation and the subsequent electrically stimulated release.

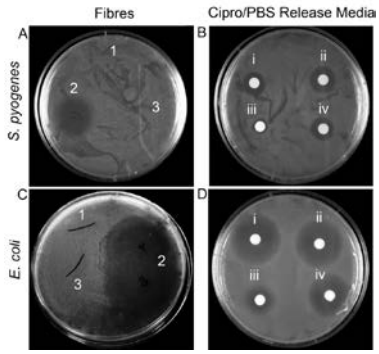

Fig. 5. Zone of inhibition (ZOI) of three different fibres (A and C) and drug release media (B and D) against *S. pyogenes* strain (A and B) and *E. coli* (C and D). (1: PEDOT:PSS-CHI-Ppy.Cl), (2: PEDOT:PSS-CHI-Ppy.Cipro), (3: PEDOT:PSS-CHI), (i: 1µg Cipro), (ii: drug release in reduced state), (iii: drug release in oxidised state), (iv: drug release in passive state). Each sample was repeated 3 times.

Moreover, zones of inhibition (ZOI) obtained using 72 h cumulative release samples against *E. coli* and *S. pyogenes* correlated well with the trend of cumulative release profiles in passive, reduced and oxidised states of the fibres (Table 2).

Table 2. Zone of inhibition resulting following application of volumes of release medium obtained under different conditions onto lawns of bacteria via paper discs. Averages of three independent experiments are shown with standard errors.

Samples	M_t/M_{tot} (%)[a]	Zone of Inhibition (mm)	
		E. coli	*S. pyogenes*
Reduced	88.0 ±14.0	26.6±0.9	14.3±0.3
Passive	47.1±1.2	27.3±0.3	14.0±1.0
Oxidised	36.5±0.5	22.7±2.8	12.0±1.2
1 µg	NA	31.3±0.6	15.0±0 0

[a.] The percentage of Cipro released was determined from the release profiles presented in Fig. 4.

3.5. Cell growth studies

Previous studies have shown that a concentration less than 150 µg/ml ciprofloxacin hydrochloride had no adverse effect on proliferation and differentiation of a variety of cell types including primary cultures of astrocytes and primary fibroblast cell lines [38, 39]. The cytotoxicity of our fibres was tested in the presence of B35 neuroblastoma cells since, the fibres are assumed to utilise for neural stimulation with controlled Cipro release. An LDH release assay was performed in the presence of a dilution series of Cipro and the results showed Cipro concentrations ≤ 125 µg/ml demonstrated any toxicity against B35 neuroblastoma cells. In addition, Cipro concentrations ≥ 250 µg/ml showed toxicity against B35 neuroblastoma cells (Fig. 6D). The presence of metabolically active cells in the presence of drug-loaded fibres was examined using Calcein AM, whereby the production of a green fluorescent product indicates living, viable cells. A counter stain (propidium iodide) was also used to indicate the presence of membrane compromised cells, indicated by red fluorescence. Following 72 h incubation, the cells surrounding the fibres were observed to show green fluorescence indicating them to be metabolically active with minimal presence of membrane compromised cells (Fig. 6A-C), similar to control glass substrates (data not shown). These results indicate the cytocompatibility of our fibres and in addition, show that the dosage of Cipro released is not high enough to cause cell mortality.

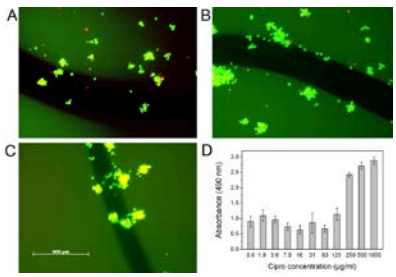

Fig. 6. B35 neural cells cultured on PEDOT:PSS-CHI (A), PEDOT:PSS-CHI-Ppy.Cl (B) and PEDOT:PSS-CHI-Ppy.Cipro (C) fibres over a period of 72 h (scale bar 800 µm). Calcein AM/PI staining renders metabolically active and membrane compromised cells bright fluorescent green and red respectively. The graph indicates the results of an LDH release

cytotoxicity assay on the effects of a dilution series of Cipro against B35 cells after 48h incubation. (D)

4. Conclusions

We have demonstrated a novel approach to produce new conducting polymer-based hybrid fibre that can be utilised as a micro-electrode for drug delivery applications. The controlled release of ciprofloxacin hydrochloride was achieved by electrical stimulation of a second conducting polymer layer. The antibacterial efficacy of the incorporated and released ciprofloxacin was confirmed against Gram-positive and Gram-negative bacteria indicating the stability of the antibiotic properties of the drug during processing and release method. In addition, neural cell culture study on the fibres showed B35 neural cells were not adversely affected by the presence of the fibres, nor any released products from the fibres.

5. Acknowledgements

The authors gratefully acknowledge the Australian Research Council for their continued financial support. The authors also wish to thank the Australian Research Council for the Federation Fellowship (Wallace), Queen Elizabeth II Fellowship (Moulton) and Australian Post-doctoral Fellowship (Razal). We also thank Mr. Tony Romeo for his invaluable assistance with SEM microscopy and EDX spectroscopy and Mr. Rouhollah Jalili for training and assistance in spinning process.

References:

[1] G.G. Wallace, S. Moulton, R.M.I. Kapsa, M. Higgins, Organic Bionics, WILEY-VCH, Weinheim, 2012.
[2] S.E. Moulton, M.J. Higgins, R.M.I. Kapsa, G.G. Wallace, Organic Bionics: A New Dimension in Neural Communications, Adv. Funct. Mater., (2012).
[3] Y. Lu, T. Li, X. Zhao, M. Li, Y. Cao, H. Yang, Y.Y. Duan, Electrodeposited polypyrrole/carbon nanotubes composite films electrodes for neural interfaces, Biomaterials, 31 (2010) 5169-5181.
[4] N.A. Kotov, J.O. Winter, I.P. Clements, E. Jan, B.P. Timko, S. Campidelli, S. Pathak, A. Mazzatenta, C.M. Lieber, M. Prato, R.V. Bellamkonda, G.A. Silva, N.W.S. Kam, F. Patolsky, L. Ballerini, Nanomaterials for neural interfaces, Advanced Materials, 21 (2009) 3970-4004.
[5] M.R. Abidian, D.C. Martin, Multifunctional Nanobiomaterials for Neural Interfaces, Advanced Functional Materials, 19 (2009) 573-585.
[6] M.R. Abidian, D.C. Martin, Experimental and theoretical characterization of implantable neural microelectrodes modified with conducting polymer nanotubes, Biomaterials, 29 (2008) 1273-1283.
[7] V. Fenik, P. Fenik, L. Kubin, A simple cuff electrode for nerve recording and stimulation in acute experiments on small animals, Journal of Neuroscience Methods, 106 (2001) 147-151.
[8] K. Yoshida, R.B. Stein, Characterization of signals and noise rejection with bipolar longitudinal intrafascicular electrodes, Biomedical Engineering, IEEE Transactions on, 46 (1999) 226-234.
[9] R. Biran, D.C. Martin, P.A. Tresco, Neuronal cell loss accompanies the brain tissue response to chronically implanted silicon microelectrode arrays, Experimental Neurology, 195 (2005) 115-126.
[10] D.-H. Kim, D.C. Martin, Sustained release of dexamethasone from hydrophilic matrices using PLGA nanoparticles for neural drug delivery, Biomaterials, 27 (2006) 3031-3037.
[11] M.R. Abidian, D.H. Kim, D.C. Martin, Conducting-Polymer Nanotubes for Controlled Drug Release, Advanced Materials, 18 (2006) 405-409.
[12] F. Unger, U. Westedt, P. Hanefeld, R. Wombacher, S. Zimmermann, A. Greiner, M. Ausborn, T. Kissel, Poly(ethylene carbonate): A thermoelastic and biodegradable biomaterial for drug eluting stent coatings?, J. Control. Release, 117 (2007) 312-321.
[13] M. Amidi, H.C. Pellikaan, A.H. de Boer, D.J.A. Crommelin, W.E. Hennink, W. Jiskoot, Preparation and physicochemical characterization of supercritically dried insulin-loaded microparticles for pulmonary delivery, EUR J PHARM BIOPHARM 68 (2008) 191-200.

[14] G.A. Buxton, N. Clarke, Drug diffusion from polymer core-shell nanoparticles, Soft Matter, 3 (2007) 1513-1517.
[15] E. Kharlampieva, V. Kozlovskaya, J. Tyutina, S.A. Sukhishvili, Hydrogen-Bonded Multilayers of Thermoresponsive Polymers, Macromolecules, 38 (2005) 10523-10531.
[16] K.S. Oh, S.K. Han, Y.W. Choi, J.H. Lee, J.Y. Lee, S.H. Yuk, Hydrogen-bonded polymer gel and its application as a temperature-sensitive drug delivery system, Biomaterials, 25 (2004) 2393-2398.
[17] T. Serizawa, D. Matsukuma, M. Akashi, Loading and Release of Charged Dyes Using Ultrathin Hydrogels, Langmuir, 21 (2005) 7739-7742.
[18] R. Wadhwa, C.F. Lagenaur, X.T. Cui, Electrochemically controlled release of dexamethasone from conducting polymer polypyrrole coated electrode, Journal of Controlled Release, 110 (2006) 531-541.
[19] D.T. Auguste, S.P. Armes, K.R. Brzezinska, T.J. Deming, J. Kohn, R.K. Prud'homme, pH triggered release of protective poly(ethylene glycol)-b-polycation copolymers from liposomes, Biomaterials, 27 (2006) 2599-2608.
[20] B.C. Thompson, S.E. Moulton, J. Ding, R. Richardson, A. Cameron, S. O'Leary, G.G. Wallace, G.M. Clark, Optimising the incorporation and release of a neurotrophic factor using conducting polypyrrole, Journal of Controlled Release, 116 (2006) 285-294.
[21] C.L. Recksiedler, B.A. Deore, M.S. Freund, A Novel Layer-by-Layer Approach for the Fabrication of Conducting Polymer/RNA Multilayer Films for Controlled Release, Langmuir, 22 (2006) 2811-2815.
[22] Y. Lin, G.G. Wallace, Factors influencing electrochemical release of 2,6-anthraquinone disulphonic acid from polypyrrole, J. Control. Release, 30 (1994) 137-142.
[23] B.C. Thompson, J. Chen, S.E. Moulton, G.G. Wallace, Nanostructured aligned CNT platforms enhance the controlled release of a neurotrophic protein from polypyrrole, Nanoscale, 2 (2010) 499-501.
[24] B.C. Thompson, R.T. Richardson, S.E. Moulton, A.J. Evans, S. O'Leary, G.M. Clark, G.G. Wallace, Conducting polymers, dual neurotrophins and pulsed electrical stimulation -- Dramatic effects on neurite outgrowth, Journal of Controlled Release, 141 (2010) 161-167.
[25] S. Sirinrath, P. Rajesh, J.W. Thomas, Electrically controlled drug release from nanostructured polypyrrole coated on titanium, Nanotechnology, 22 (2011) 085101.
[26] D. Svirskis, J. Travas-Sejdic, A. Rodgers, S. Garg, Electrochemically controlled drug delivery based on intrinsically conducting polymers, Journal of Controlled Release, 146 (2010) 6-15.
[27] J.H. Johnston, J. Moraes, T. Borrmann, Conducting Polymers on Paper Fibres, Synthetic Metals, 153 (2005) 65-68.
[28] R. Jalili, J.M. Razal, P.C. Innis, G.G. Wallace, One-Step Wet-Spinning Process of Poly(3,4-ethylenedioxy-thiophene):Poly(styrenesulfonate) Fibers and the Origin of Higher Electrical Conductivity, Advanced Functional Materials, (2011) n/a-n/a.
[29] J. Ouyang, C.W. Chu, F.C. Chen, Q. Xu, Y. Yang, High-Conductivity Poly(3,4-ethylenedioxythiophene):Poly(styrene sulfonate) Film and Its Application in Polymer Optoelectronic Devices, Advanced Functional Materials, 15 (2005) 203-208.
[30] X. Crispin, F.L.E. Jakobsson, A. Crispin, P.C.M. Grim, P. Andersson, A. Volodin, C. van Haesendonck, M. Van der Auweraer, W.R. Salaneck, M. Berggren, The Origin of the High Conductivity of Poly(3,4-ethylenedioxythiophene)−Poly(styrenesulfonate) (PEDOT−PSS) Plastic Electrodes, Chemistry of Materials, 18 (2006) 4354-4360.
[31] H. Okuzaki, Y. Harashina, H. Yan, Highly conductive PEDOT/PSS microfibers fabricated by wet-spinning and dip-treatment in ethylene glycol, European Polymer Journal, 45 (2009) 256-261.
[32] A.J. Granero, J.M. Razal, G.G. Wallace, M. in het Panhuis, Spinning Carbon Nanotube-Gel Fibers Using Polyelectrolyte Complexation, Advanced Functional Materials, 18 (2008) 3759-3764.
[33] J. Ouyang, Q. Xu, C.-W. Chu, Y. Yang, G. Li, J. Shinar, On the mechanism of conductivity enhancement in poly(3,4-ethylenedioxythiophene):poly(styrene sulfonate) film through solvent treatment, Polymer, 45 (2004) 8443-8450.

[34] J.M. Nelson, T.M. Chiller, J.H. Powers, F.J. Angulo, Fluoroquinolone-Resistant Campylobacter Species and the Withdrawal of Fluoroquinolones from Use in Poultry: A Public Health Success Story, Clin infect dis, 44 (2007) 977-980.
[35] A. Dalhoff, W. Weidner, Diffusion of ciprofloxacin into prostatic fluid, European Journal of Clinical Microbiology & Infectious Diseases, 3 (1984) 360-362.
[36] T.W. Lewis, S.E. Moulton, G.M. Spinks, G.G. Wallace, Optimisation of a polypyrrole based actuator, Synthetic Metals, 85 (1997) 1419-1420.
[37] R.T. Richardson, B. Thompson, S. Moulton, C. Newbold, M.G. Lum, A. Cameron, G. Wallace, R. Kapsa, G. Clark, S. O'Leary, The effect of polypyrrole with incorporated neurotrophin-3 on the promotion of neurite outgrowth from auditory neurons, Biomaterials, 28 (2007) 513-523.
[38] A. Gürbay, C. Garrel, M. Osman, M.-J. Richard, A. Favier, F. Hincal, Cytotoxicity in ciprofloxacin-treated human fibroblast cells and protection by vitamin E, Human & Experimental Toxicology, 21 (2002) 635-641.
[39] A. Gürbay, B. Gonthier, L. Barret, A. Favier, F. Hincal, Cytotoxic effect of ciprofloxacin in primary culture of rat astrocytes and protection by Vitamin E, Toxicology, 229 (2007) 54-61.